Computers in Orthodontic Research

4

Demetrios J. Halazonetis

4.1 Introduction

Orthodontic research is no exception to the widespread application of computers. Computers are used at almost all stages of a scientific research project, from submission of a proposal (word processing) to collection of data (measuring and statistical processing) to presentation at meetings and final publication (word processing and slide presentation). This chapter focuses on the more specialised uses of computers in orthodontic research, in an effort to reveal the advantages that they offer, but also to point out their limitations. Due to the continual advancement of hardware and software, the information presented here is certain to become outdated very quickly. Emphasis will therefore be placed on the basic principles, so that the reader will be able to appraise current techniques as well as new developments.

4.2 Measuring Diagnostic Records

Measuring is the basis of all scientific research. Orthodontics may well be the most measurement-preoccupied specialty in dentistry. Since the advent of cephalometrics in the early 1930s and its flourishing in subsequent decades, there are very few published clinically oriented papers that do not include some cephalometric measurements. These are currently performed mainly by computer software on scanned images or on digital radiographs. Any measurement potentially includes sources of error, and cephalometrics is no exception. Studies analysing cephalometric errors have been reported in the literature [1–8], but they mainly deal with human error, presuming that computers are mathematically accurate and precise and do not make

D.J. Halazonetis
Department of Orthodontics, School of Dentistry,
University of Athens,
6 Menandrou Street, Kifissia 14561, Greece
e-mail: dhal@dhal.com

T. Eliades (ed.), *Research Methods in Orthodontics*,
DOI 10.1007/978-3-642-31377-6_4,

mistakes. Although this may be true, it is only under the condition that computers are appropriately used. Unfortunately, unfamiliarity with the internal workings of computers, scanners and other devices is not uncommon and may lead to compromised results. Also, special features and capabilities of computer-aided measurement methods may not be appreciated and go underused. These topics are discussed below and apply both to cephalometric radiographs and other diagnostic records that can be measured in similar ways, such as facial photographs, dental casts, panoramic radiographs, animal radiographs and histological preparations.

Before discussing the above issues, it may be appropriate to review a few definitions pertaining to measurements and errors. The following terms will be used:

Precision or Repeatability: the degree to which the measurement has the same value when measured several times. It is assumed that the same examiner performs the measurements, so this is also known as intra-examiner reliability.

Reproducibility: the degree to which the measurement has the same value when measured by different operators, also known as inter-examiner reliability.

Reliability (inter- and intra-examiner) is assessed by repeated measurements. The variance of the repeated measurements shows the amount of random error. Possible bias between a first and second measurement is revealed by testing the difference between the replicated measurements.

Validity or Accuracy: the degree to which the measurement actually represents what it was intended to represent, that is, is close to the 'true' value. Note that validity in identification of cephalometric landmarks cannot be assessed by repeated tracings, either by one or more observers, because there is no "gold standard" against which to compare the observers' judgments. One method to test validity is to place markers on anatomical structures of skulls and compare their positions, as seen on a cephalogram, with the corresponding cephalometric points, as located without the markers. Such studies have reported validity errors for several commonly used points, both skeletal and dental [9, 10].

4.2.1 Digitisers

Computer-aided cephalometric software has been widely available since the introduction of personal computers. Early implementations relied on a digitiser to get the coordinates of the points directly from the radiograph or from its tracing, and only relatively recently have scanners or digital radiographs been introduced. Digitisers have now been almost completely phased out, so only a brief section will be devoted to them.

Digitisers are electromagnetic devices that detect the position of a cross hair pointer on a tablet by means of electromagnetic fields. For this reason, a certain amount of interference from external fields or metal objects is expected. Accuracy is reported to be approximately 0.1 mm, although values differ between various

models and manufacturers. Studies assessing digitiser accuracy [11, 12] have found both systematic and random errors, but the total errors are not large, at least when compared to more serious error sources, such as the error of landmark identification.

Digitisers can be used either directly on the radiograph or indirectly on a tracing of the radiograph. Direct use requires a digitiser with a translucent surface, so that the radiograph can be lit from underneath. This is the recommended procedure, as it is considered to exhibit smaller errors, because there is no need for the intermediate step of creating a tracing [3, 6].

The major benefit of using digitisers is that the radiograph is inspected directly by the human eye, thus taking advantage of the capabilities of this organ. A very important capability, when viewing a radiograph for landmark identification, is the power to discriminate between different shades of grey. The human eye has a rather limited power in this respect, being able to discern approximately 30 grey levels. However, this is coupled with an extraordinary ability to accommodate to a very wide range of light intensities (of the order of 10^{10}) by adaptation mechanisms, such as the opening and closing of the iris and the different sensitivities of the photoreceptors. At each adaptation level, there are limited intensities that can be discerned, but as the observer scans the radiograph, the eye changes its accommodation level, in effect extending the total range of grey levels detected [13]. To facilitate accommodation, careful control of the ambient light is essential when viewing radiographs. Also, masking around the region of interest is helpful, because it excludes light from neighbouring areas, which may affect the adaptation level.

4.2.2 Scanners

Scanners digitise an image by shining light on it and reading the reflected or transmitted light, using a light-sensitive element (usually a charge-coupled device, CCD). In the case of radiographs, the light source is typically placed on a cover above the radiograph (the light transparency unit), and the CCD scans the radiograph from underneath. The intensity of the transmitted light is converted to a digitised signal that constitutes the image of the radiograph. Scanners have certain characteristics that determine the quality of the image [14]. These are resolution, colour depth and optical density. Ensuring a good image is paramount to precise measurements.

4.2.2.1 Resolution

Resolution refers to the number of pixels of the resulting image. Resolution is usually measured in dots per inch (dpi) and can extend above 1,200 dpi. It is important to differentiate between the optical resolution of the scanner and the total resolution. The optical resolution is determined by the number of elements of the CCD and the step size of the motor that moves the CCD. These factors commonly allow resolutions of 600–1,200 dpi. Software interpolation can then be applied to increase the resolution to much higher values. However, this increase is, in essence, guesswork and does not represent actual information gathered from the image.

The optimum resolution for scanning cephalometric radiographs is an important consideration [15]. The decision is usually a compromise between the need for sufficient detail to identify landmarks and practical aspects of computer speed and storage. Conventional cephalometric measurements have many sources of error, the most significant being the error of point identification (see below), which is of the order of millimetres (mm). Therefore, a resolution that will give a few pixels per mm would be sufficient for most purposes. Simple calculations show that resolutions of 150–300 dpi result in 6–12 pixels/mm, which should be more than enough. No significant benefit has been shown for 600 dpi as compared to 300 dpi [16]. Indeed, resolutions as low as 75 dpi have been regarded as sufficient [17], but this conclusion was reached with an experimental setup that did not allow zooming of the image, thus negating the increased detail of higher resolutions (see below).

4.2.2.2 Colour Depth

Colour depth corresponds to the number of bits dedicated to each colour of the image. Computer colour images are composed of three primary colours (red, green and blue). These colours are mixed in different proportions (intensities) to produce all the different colours of the image. The intensity of each of the primary colours is described by a number. The computer usually assigns one byte (8 bits) to represent each primary colour, so most computer images are 24-bit images. A single byte can describe 256 different levels of intensity, so a 24-bit colour image can contain $256 \times 256 \times 256$ different colours (approximately 17 million). Note that shades of grey need equal amounts of the primary colours, so greyscale images can be represented by one byte instead of three and contain a maximum of 256 shades of grey. Higher-level machines and scanners can use more bits per colour (12 or 16 bits) to describe more shades of grey (4,096 or 65,536). However, most computer screens can display only 8 bits per colour, so even if the image is a 16-bit greyscale image, it will be converted into 8 bits in order to be displayed.

High-bit images (12 or 16 bits) seldom offer substantial benefits for orthodontic research purposes [18]. One reason for this is the inability of conventional monitors to display high colour depth. Another is the inability of the human eye to detect very fine gradations in light intensity. It should be pointed out that 12- or 16-bit greyscale images are used effectively in computed tomography (CT) images. In such images, either the greyscale range can be compressed to 8 bits for display of the whole dataset or only a part of the extended range can be selected. By choosing to view the high intensity pixels, the bony tissues are made visible, whereas the soft tissues can be displayed by selecting the lower range. This procedure is commonly known as windowing.

4.2.2.3 Optical Density

Optical density refers to the range of light intensities that a scanner can acquire. This depends on the capabilities of the CCD and the electronics of the scanner. It is expressed in a logarithmic scale and typically ranges from 2.4 to 4.2 for consumer scanners on the market.

Assume that a radiograph is being scanned. Light of a particular intensity falls on the radiograph, and part of this is transmitted through it and reaches the CCD. The ratio of transmitted light to incident light at a particular location of the radiograph is the transmittance. The inverse of this ratio is the opacity. The logarithm of opacity is the optical density of the radiograph:

$$\text{Density} = \log_{10}(\text{opacity}) = \log_{10}\left(\frac{\text{incident light}}{\text{transmitted light}}\right)$$

In the case of photographs, where the incident light is reflected, opacity is defined as the ratio of incident over reflected light.

Dark areas of a radiograph transmit very little of the incident light, so they have a large optical density, whereas light areas are almost completely transparent and have a small density. The difference between the smallest and largest density is the density range. The density range of a radiograph may extend from 3.4 to 4.2 or more, signifying that the intensity of light passing through the brighter areas is more than 15,000 times higher than the intensity of light going through the dark areas. In contrast, the density range of a printed image is much lower, because light is reflected and not transmitted through it. Photographs and printed images seldom have a density range that exceeds 2.4. Scanners can capture a limited density range. The lower-priced models have a range of approximately 2.4, which is adequate for photographs and other printed documents, but insufficient for slides or radiographs. When the density capabilities of the scanner are insufficient, the brighter part of the image is given priority, and the darker areas are captured as a uniform blackness. This results in obliteration of the detail in dark areas, such as, for example, the hyoid bone area in lateral cephalograms.

Density values should be at least 3.4–3.6 for adequate results, values achievable by high-end flatbed scanners. Figure 4.1 shows the same image acquired from two

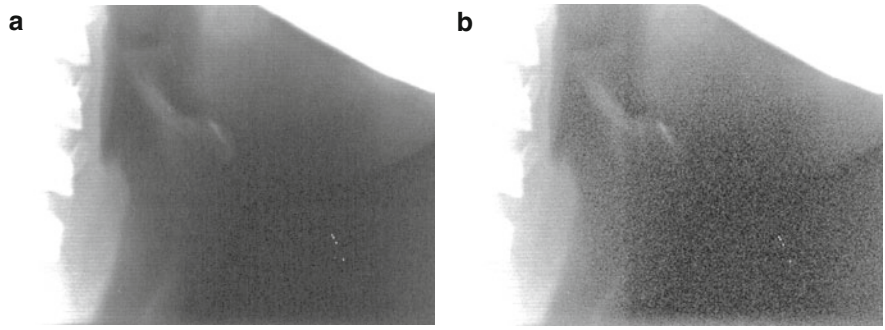

Fig. 4.1 The area of the hyoid bone scanned (**a**) with the Epson 1600 Pro (optical density 3.3) and (**b**) the Epson 1680 Pro (optical density 3.6). Note the reduced noise level and the significantly better detail capture from the scanner with the higher density. Both images have been processed by adjusting gamma so that dark areas are more apparent. For this reason, the mandible and vertebrae appear "washed out"

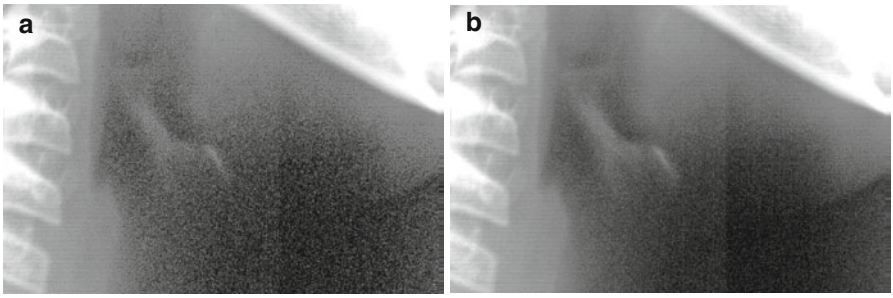

Fig. 4.2 (**a**) The hyoid bone area, scanned once, with a scanner of optical density 3.3. Notice amount of random noise. The image has been manipulated by changing the gamma value, so that dark areas are enhanced. (**b**) The same area, produced after scanning four times and merging the results

scanners, one with optical density of 3.3 and the other with optical density of 3.6. (Note that because of the logarithmic scale used in expressing optical density, the better of these two scanners can discern twice the range than the other one.) Both images have been enhanced by the same amount to show the difference in the detail of the dark areas. Optical density is perhaps the single most important factor that determines the quality of a scanned radiographic image.

4.2.2.4 Noise

Noise is another factor that degrades scanned images [19]. Noise appears as random variations in image intensity at the pixel level and is most evident in the dark areas of the image. Because noise is random, it can be reduced substantially by multiple scanning. This technique scans the radiograph more than once and averages the results. Due to the random nature of noise, the average of multiple scans will tend to cancel out noise and retain the true value. High-end scanners are capable of acquiring multiple values for each pixel and take the average during a single pass. If this feature is not available, it can be done by software, but then multiple passes are required. Figure 4.2 compares the same area scanned once and four times. Noise reduction is evident.

4.2.3 Digital Radiography

Digital radiographic machines register the intensity of the radiation transmitted though the patient's head by an electronic sensor and convert it directly to a digitised signal, thus eliminating the intermediate steps of developing a film and digitising it with a scanner. The sensor is a charge-coupled device (CCD). Most sensors have small dimensions and it is not possible to cover the whole area of interest. To solve this problem, the manufacturers use an array of sensors, arranged side by side. The array extends along the required width and is moved vertically during the exposure, in tandem with the x-ray source, to scan the whole head (horizontal scanning is also available). This method presents certain differences in comparison to the conventional approach:

1. A longer exposure is needed, because of the movement of the source and sensor array. This requires the patient to remain still for a number of seconds (exposure times differ between machines) and may introduce errors due to movement of the head or changes in posture of the soft tissues, including the tongue and soft palate. Some systems are capable of acquiring a cephalometric digital image without scanning ("one shot") and overcome the disadvantages of long exposure.
2. Even though a longer exposure is used, total radiation exposure is reduced, due to higher sensitivity of the sensor array and the fact that only a thin stripe is radiated at any one time.
3. Beam geometry may be different, resulting in a different magnification pattern. The conventional (non-digital) systems use a beam that diverges from a single point towards all directions, to produce a cone-shaped geometry. This results in symmetrical magnification of the exposed structures around the central beam. In contrast, some digital systems use a fan-shaped beam that scans the patient vertically (or horizontally) in a parallel fashion. Therefore, magnification is present only along the horizontal (or the vertical) axis [20]. This problem has been overcome in newer machines that incorporate rotational movement of the x-ray source, or movement of a slit diaphragm, thus producing comparable magnification to conventional systems.

Other digital systems use a hybrid method to acquire the image. A special phosphor storage plate (PSP), similar to a conventional film, is used to obtain the image, by means of conventional x-ray equipment. The plate is then inserted into a special scanner, and the captured image is converted to a digital file.

4.3 Advantages and Capabilities of Computer-Aided Cephalometrics

The advantages of using a computer for performing cephalometric measurements are so significant that probably no research is being conducted by manual methods any more. The obvious speed factor is especially important when a large number of diagnostic records need to be processed [21, 22]. Ease of use is also important, because it relieves the operator of fatigue. However, these are secondary benefits. Error control, a major problem in any investigation, is where computer-aided cephalometrics should focus. Reducing both random and systematic errors is not an easy task. Several methods are discussed below, but it should be noted that very limited data are available regarding their effectiveness. Most recommendations are based on logical deductions and assumptions, and further studies are needed for validation.

4.3.1 Error Control

Errors in cephalometric analysis have been extensively discussed in the orthodontic literature [1–8]. It is a common conclusion that error of point identification is the most significant source. Computers may help in reducing this error by the following methods:

4.3.1.1 Image Enhancement

Various image manipulations can be applied to make some areas more conspicuous and aid in visualisation. Contrast, brightness and gamma can be adjusted, and histogram techniques can be applied over the whole image or at specific areas [13], as shown in Fig. 4.3.

4.3.1.2 Multiple Digitisation

Multiple digitisation has been recommended as a method to reduce point identification error [2, 23]. Baumrind and Miller [23] reported that in order to reduce this error by half, each point should be digitised four times, and the average of the four attempts should be used as the location of the point. Although this may be excessive [4], even a double digitisation is not possible without a computer system. Cephalometric software allow multiple digitisation on screen (without showing the previous attempts, so as not to bias the user) and calculate the average position. The user can inspect the digitisations and delete outliers. Multiple digitisation may be more important in case reports than large-scale studies, where errors tend to average out [2].

4.3.1.3 Magnification of the Image and Precision Limitations

The scanned image can be magnified on-screen to almost any detail in order to facilitate point placement. The limiting factor here is the resolution at which the radiograph was scanned. As mentioned earlier, a resolution of 150 dpi will produce approximately 6 pixels per mm, which far exceeds the usual requirements of cephalometrics.

The precision with which points are located on-screen depends on a number of factors, such as scanning resolution, the zoom setting when digitising and the internal design of the software [15, 24]. The important thing to keep in mind is that the points are located using the mouse, so the movement of the mouse on screen is a major factor in determining the precision. For example, assume that a radiograph is displayed at approximately life size on a computer monitor. Assume a 15″ TFT monitor running at a resolution of 1,024×768 pixels with physical dimensions of 304×228 mm. The dimensions of a screen pixel are easily calculated as 0.297×0.297 mm. Since the mouse can only move from pixel to pixel on the screen, it becomes evident that it is not possible to digitise points with more precision than approximately one-third of a millimetre. If the radiograph is zoomed out to occupy less screen space, this value will worsen. If more detail is required, the software should allow zooming. Assume that the image is zoomed in so that 10 mm is now displayed at a size of 10 cm on screen. This should allow digitisation at an accuracy of 0.03 mm. However, two other factors come into play at this magnification. One is the resolution used during scanning. If this was relatively low, then the image pixels will be apparent, setting a limit to the effective precision; although we can place the mouse and digitise at sub-pixel positions of the image, there is no way to ensure that the digitised location is correct. The final limiting factor is the internal design of the software program, which may not allow unlimited precision.

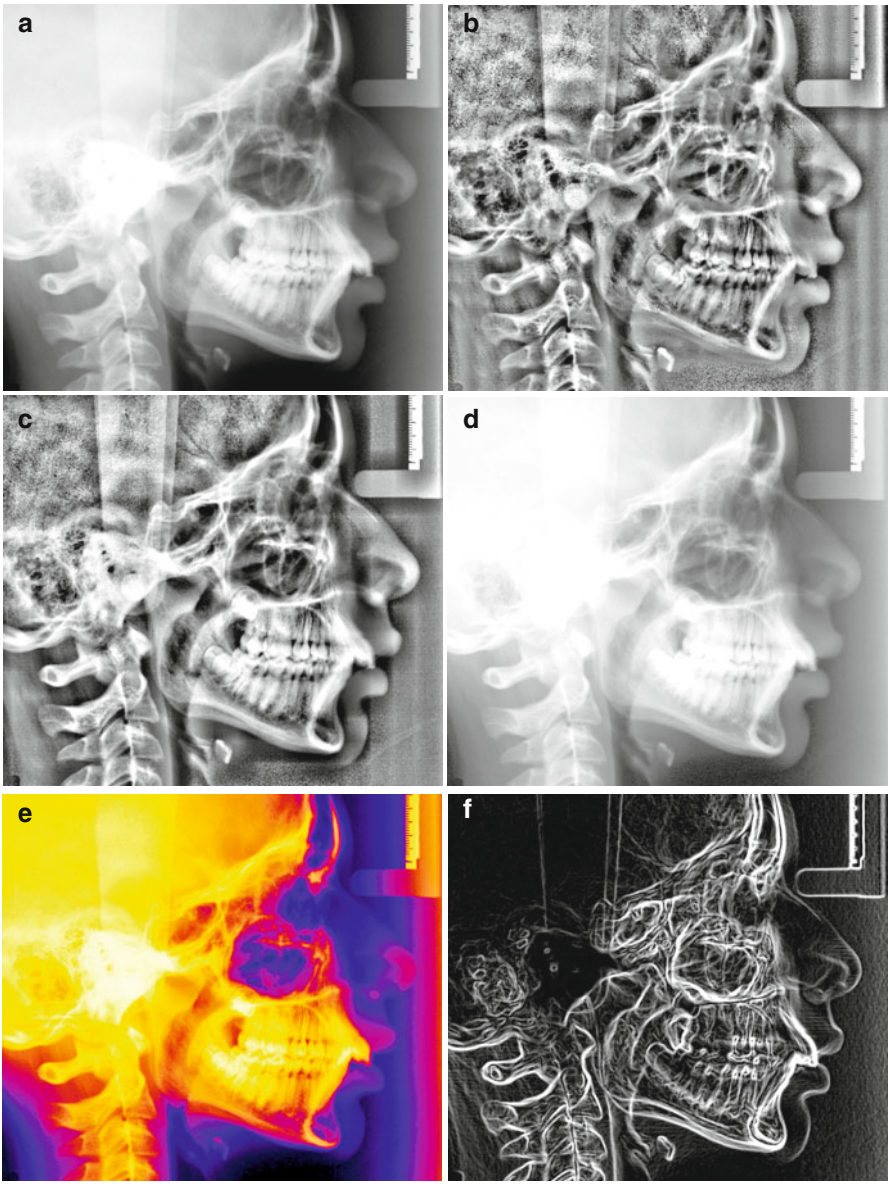

Fig. 4.3 Results of manipulation procedures: (**a**) original image, (**b**) adaptive histogram equalisation, (**c**) adaptive levels, (**d**) gamma adjustment, (**e**) colourisation and (**f**) edges

A practical method to calculate the maximum precision under specific conditions is the following:

1. Calculate the precision offered by the scanning procedure. This is equal to 25.4 divided by the resolution in dpi (1 in. is 25.4 mm). So a resolution of 150 will offer a maximum precision of approximately 0.17 mm.
2. Calculate the precision offered by the screen and zoom factor. First, divide the physical width of the computer screen by the number of pixels to get the size of each pixel. Then adjust by the zoom value. For example, if the screen is 304 mm in width and is running at a resolution of 1,024×768 pixels, the pixel size is 0.297 mm. This is the maximum precision if the radiograph is viewed at life size. For double than life size, divide the number by 2 to get 0.148 mm. For ten times life size, the precision is 0.0297 mm.
3. The final precision is the worse of the results calculated in steps 1 and 2 above. Check this with the data given by the software manufacturer, because the software itself may set limits, due to internal number representation or other design factors.

4.3.1.4 Automatic Point Location

One of the reasons that the error of point identification is high for points such as Gonion and Gnathion is that these points are located on curved osseous boundaries. The investigator has the task of locating the most extreme point along this boundary (e.g. the most inferior and posterior point, in the case of Gonion), not an easy task given the absence of anatomical markers. Geometrical constructions can be used as aids, but these may also introduce errors of their own. An alternative is to delegate the task to the computer. Software already exists that can assist in this respect. The user need only draw the outline of the boundary, and then the software automatically locates the points on this boundary following simple geometrical rules of point definition.

As an example, Fig. 4.4 shows the placement of points along the outline of the mandibular symphysis. The computer locates each point according to its definition; Pogonion is placed at the most anterior position, Menton at the most inferior, etc. The anteroposterior direction is defined by the Frankfurt horizontal plane, which has been digitised previously, thus circumventing errors caused by improper head orientation.

Automatic location of points on digitised outlines may remove some of the subjectivity, and therefore error, of point identification, but it may introduce a new source of error, that of tracing the outline. However, because the outline usually represents a well-defined brightness edge in the radiographic image, it is possible to use computer vision techniques to identify it. Edge-detection methods [13, 25] are among the first developed methods in computer vision, and, although not as reliable as one would like, they can be used to good effect. Such methods have only recently been introduced in cephalometric software, and their effectiveness in error reduction is beginning to be investigated [26].

4.3.2 Magnification Adjustment

A common problem with orthodontic research studies is that the cephalometric radiographs may have been acquired by different x-ray machines, each possessing a different magnification factor. Although angular measurements are not affected,

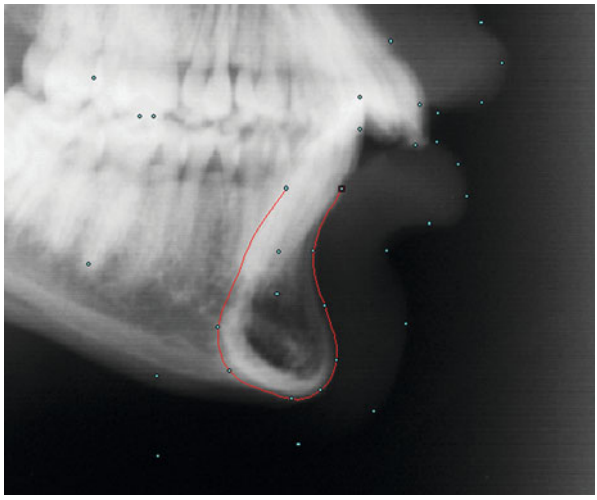

Fig. 4.4 Automatic placement of points at the mandibular symphysis. The user has drawn the outline of the symphysis (*red line*) and the computer automatically places each point (*cyan dots*) on this outline, according to predefined geometrical relationships. The Frankfurt horizontal plane (not shown) is used to establish the reference horizontal. Other digitised points are also shown

linear measurements need to be rescaled to a common magnification for proper comparison. The aspect of different magnification between different machines is also important when assessing linear measurements of a patient in comparison to published standards. Correction to natural size is recommended, in order to avoid confusion and obtain valid results [27].

Differences of magnification present larger problems in superimpositioning. If the original and final cephalometric radiographs of a patient have been taken on machines with different magnification, it is not possible to superimpose them manually, unless one resorts to such creative measures as enlargement or reduction of the tracings by photocopying. The use of computers can help in this respect. All tracings can be rescaled to the same magnification (or to life size), thus enabling correct superimpositioning.

4.3.3 Structural Superimposition

Superimposition of radiographs on internal osseous structures is recommended for assessing treatment or growth changes [28]. This is not easy to accomplish manually because a lot of structures need to be traced and precision may be compromised. Computers allow direct superimpositioning of radiographic images using different colours for each (Fig. 4.5). When two structures align, the colours are blended together to produce a different colour. This facilitates the procedure significantly. Automated methods that aim to superimpose anatomical structures so that the optimum alignment is achieved are currently in the experimental stage.

4.3.4 Morphometrics

The field of morphometrics [29–32] is relative new in biology and has only recently been applied to orthodontics [33–38]. Morphometrics aims to overcome some of the fundamental problems of conventional cephalometrics [39], such as the problem of

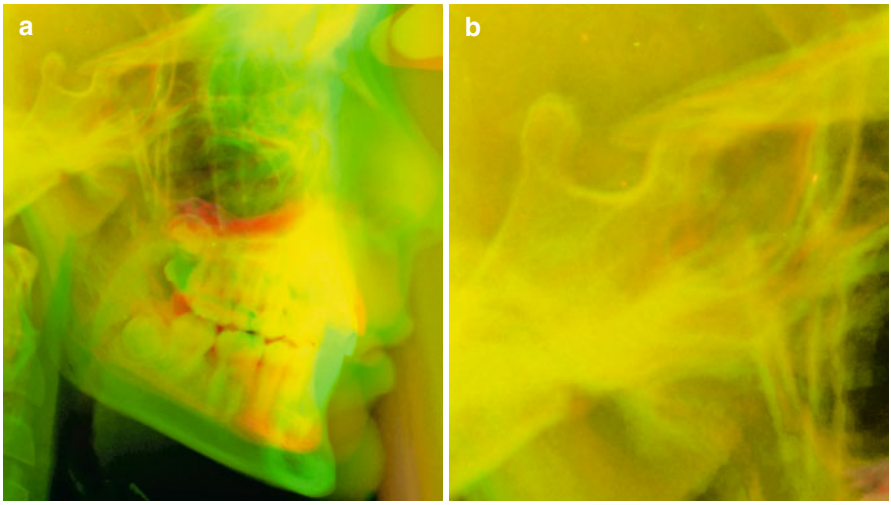

Fig. 4.5 (**a**) Structural superimposition of before and after radiographs on anterior cranial base. The radiographs have been colourised to *red* and *green*; aligning structures are yellow. (**b**) Detail of the sella area

separating size from shape, selecting an appropriate superimposition scheme and interpreting the results of the measurements. Morphometric methods require extensive calculations that are not feasible without computer assistance. Cephalometric software are now available that can perform Procrustes superimposition and calculate principal component analysis and other morphometric procedures. Detailed explanation of such methods is beyond the scope of this chapter.

4.3.5 Warping of Images

Computer graphics have advanced to the point that it is now easy to modify images by deforming them and blending them in a controlled manner to create realistic pictures of objects that do not exist. Such effects have been applied successfully in the movie industry and have also found application in orthodontics. Two terms are coined for such procedures [40, 41], but they are sometimes used interchangeably in the literature: "Warping" refers to the deformation of a single image, and "morphing" refers to the deformation of two images and the creation of a new image by blending the two warped images together. Morphing can be used to generate smooth transformations from one image to another and is most often used for the creation of animated sequences [41]. In orthodontics, such movies are used to show simulations of treatment, by depicting a smooth transition from the initial photograph of a case to the final result (Fig. 4.6). The impact to a prospective patient is significant, because treatment procedures can be explained and presented in a highly visual manner.

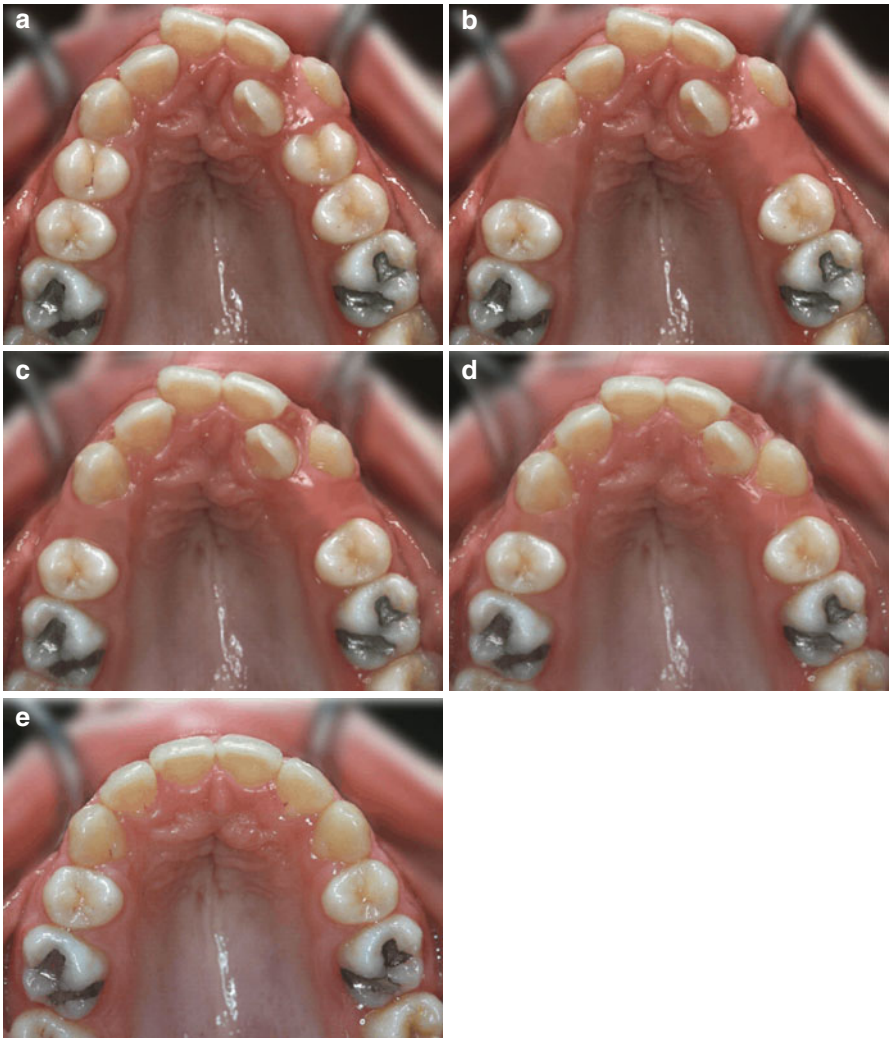

Fig. 4.6 Series of images used for the creation of a morphing movie that shows a simulation of orthodontic treatment. The only real images are the initial (**a**) and final (**e**) ones. Image (**b**) was created from (**a**) by digitally deleting the premolars. Intermediate images (**c**, **d**) were constructed by morphing between images (**b**, **e**)

The technique of warping is used for creating photorealistic treatment predictions of the patient's face. Instead of drawing a prediction tracing from a lateral cephalogram to show how the facial profile may look after a surgical procedure, it is now possible to use the pretreatment profile photograph of the patient as the starting point. The photograph is warped (deformed) so that the facial outline takes the shape of the predicted outline. Various mathematical procedures exist for such deformations [42, 43]. The result has been found to

enhance patient–doctor communication [44], but the diagnostic value is debatable, due to the following reasons:

1. The warped image is based on the cephalometric prediction of the facial outline. Thus, the final result is no more accurate than the cephalometric tracing.
2. The warped image is based on the initial pretreatment photograph. The photograph is warped so that the facial outline changes shape and becomes the same shape as the tracing prediction. In this process, the remainder of the face is also deformed, not according to any biological model, but based on mathematical algorithms. This deformation will not reflect the true changes that are produced by treatment, even if the final facial outline has been accurately predicted. Orthodontic and surgical treatments have effects on the lateral aspects of the face (cheeks, nose, mandibular outline, etc.) that cannot be predicted by this method.

In addition to clinical applications, warping and morphing have found increasing use in research [45–50]. Until recently, studies on facial attractiveness and investigations on facial symmetry, facial shape and skin texture have been limited, because they were conducted using drawings or silhouettes, and the investigation of the subtle effects of the many confounding variables was not possible. The computer opens up a large array of possibilities, enabling us, in an experimental setting, to control, manipulate and test each parameter individually. Starting from an original photograph, we can deform it or blend in other photographs and thus change the texture of the skin, the shape of the facial outline (in profile and frontal view), the shape of the internal facial components (e.g. the shape of the eyes, the mouth or the nose), the configurational arrangement of the internal components, their colours, the hair style and a number of other features [51]. This process leads to the creation of novel photorealistic faces that can be used for testing purposes or for education (Fig. 4.7). This is a young area of research but it is growing rapidly, because the questions addressed are not limited to orthodontics but extend to aesthetics, plastic surgery, facial perception and other fields.

4.4 Three-Dimensional Records

Although cephalometric radiographs are the main research source in orthodontics, other diagnostic records can be assessed in a similar manner. Facial photographs, photographs of dental casts, other radiographs (e.g. panoramics, hand/wrist) and animal records – anything that can be entered into the computer as an image – can be measured and analysed.

Three-dimensional records are utilised in increasing frequency, driven by advances in computer hardware and software and by the recognition that two-dimensional records are inherently limited in their ability to document the 3D craniofacial structures and the dentition. Since the beginning of orthodontics, the only 3D orthodontic records have been the study casts. The ideal goal in orthodontic diagnosis would be to replace all two-dimensional records (cephalometric and panoramic radiographs, facial and intraoral photographs) with three-dimensional ones. The diagnostic procedure and treatment planning (measurements and treatment prediction) would take

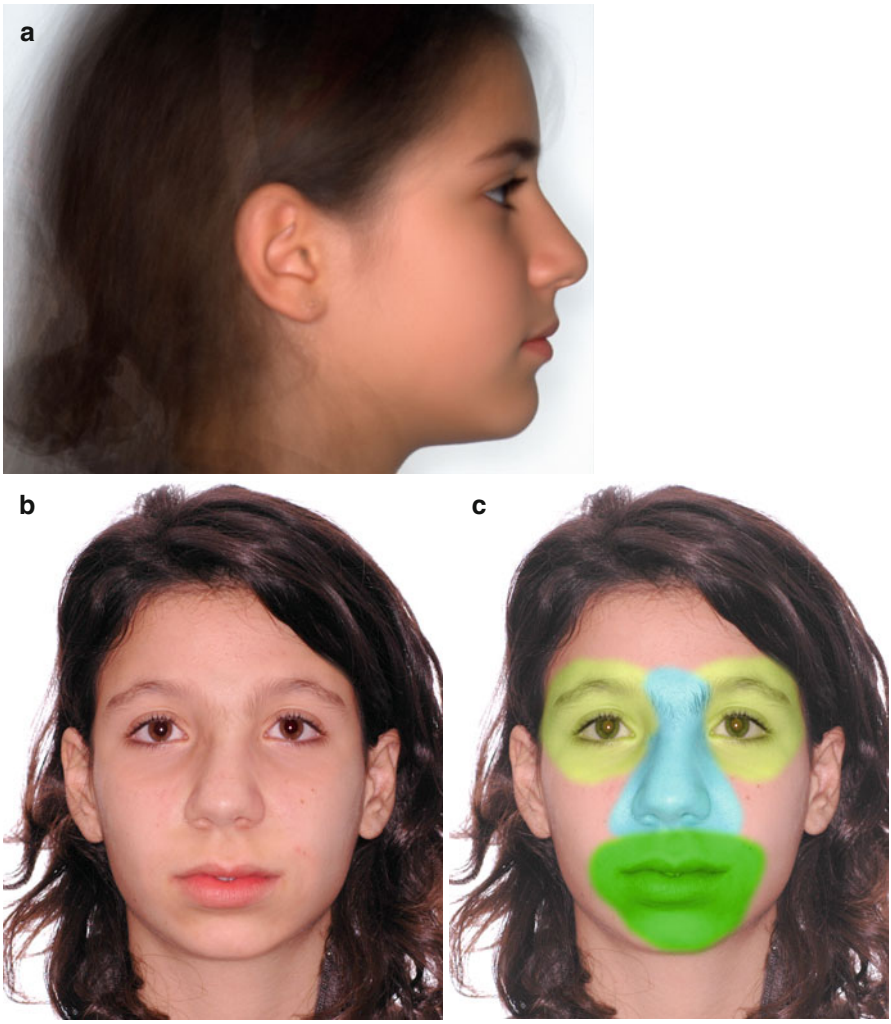

Fig. 4.7 (**a**) Average face created by merging the warped photographs of 20 patients. Photographs were warped to a common shape before merging so that corresponding facial features would superimpose closely. Warping was not applied to the hair area, and area is blurred. Average faces have been found to be highly attractive, when compared to the original faces from which they were created. (**b**) Virtual face created from a composite of face parts taken from four subjects. (**c**) Colourised areas show the parts that were taken from other subjects and merged with the underlying face. The left eye is identical to the right eye but flipped

place directly on the 3D records, thus circumventing many of the current limitations. Orthodontic 3D records aim at acquiring the geometry of three different parts of the craniofacial complex: the skeletal structures, the soft tissue surface of the face and the dentition. These components present different problems regarding methods of acquisition, because of differences in their material nature and the required accuracy.

4.4.1 Skeletal Structures

Acquisition of the 3D geometry of the craniofacial skeleton has been a mainstream application for several years now. The evolution of CT scanners and related software has enabled detailed imaging of the skeleton, but orthodontic applications have been limited to complex craniofacial problems that are seldom encountered in mainstream clinical practice. The main problems of CT scanning are the cost of the procedure and radiation exposure.

4.4.1.1 Radiation

Radiation risk is commonly assessed by the "effective dose". The effective dose is the sum of the doses to each organ exposed to the radiation, weighted by a coefficient, which represents the organ's sensitivity to radiation exposure. Organs such as the gonad and bone marrow have high weighting factors, whereas skin and neural tissue have low weighting factors. The unit of effective dose is the Sievert (Sv). For dental applications, where dose is low, the mSv (1,000 mSv = 1 Sv) and the μSv (1,000 μSv = 1 mSv) are used.

Due to exposure to natural radiation (from the earth minerals, from cosmic radiation, and from radiation within the human body), it is estimated that an individual receives about 3,000 μSv/year. A typical conventional CT scan of the whole head will incur an effective dose of about 2,000 μSv, which is equivalent to 8–12 months of background radiation. In comparison, a cephalometric radiograph entails a dose of about 5 μSv, and a panoramic gives approximately 25 μSv [52–56]. These values show that dental radiography involves low radiation exposure, but incorporation of 3D CT records as a routine orthodontic procedure would increase the dose substantially [57]. Cone-beam computed tomography (CBCT) results in a wide range of effective dosage to the patient, depending on the machine and the parameters of the examination, including field of view size and image resolution. Typical dosage ranges from 70 to 370 μSv [58]. Guidelines for CBCT imaging in dentistry have been established by national societies and a European initiative [59, 60].

4.4.1.2 Accuracy

The diagnostic value of 3D records is directly related to their validity and precision. The validity of CBCT records has been reported in a number of investigations, by comparing measurements taken from the 3D reconstructions of skulls or cadaver heads with direct measurements using callipers or 3D digitisers [61–70]. It is generally accepted that CBCT measurements are valid and accurate, but the threshold used for 3D reconstruction and demarcation of tissues may be a significant factor that needs attention.

The choice of the threshold for reconstruction and measurement is difficult because tissues may appear more or less dense than expected, depending on the area being examined and the effect of artefacts. Among the most significant artefacts in CBCT imaging are noise, the partial object effect and the partial volume averaging effect [71, 72]. Noise is present due to reduced x-ray energy, purposely set low on CBCT machines in order to reduce patient exposure. The partial object effect arises

because the field of view is smaller than the object under investigation; the parts of the patient's head that lie outside the field of view may significantly alter the density of the voxels, causing inconsistencies between tissue density and voxel density. These inconsistencies do not allow a reliable correspondence between voxel density and Hounsfield values and thus do not allow reliable differentiation between tissues, based solely on voxel values [73–75]. The partial volume averaging effect is evident when the voxels are large relative to the size of the object under investigation, resulting in multiple tissues occupying the space of a single voxel. In such cases, the value of the voxel will represent the average of the multiple tissues, giving a false impression of the voxel's composition.

From the above it is evident that a global threshold for tissue segmentation and measurement may not be appropriate [76]. Especially prone to systematic errors are thin structures, such as the alveolar covering of incisor roots. Due to reduced resolution of CBCT images [77], alveolar bone is consistently underestimated and dehiscences and fenestrations are significantly overestimated [78–81]. However, high-contrast globular structures, such as teeth, also show errors in measurement which may exceed 1 mm, even if images are taken under ideal conditions, mainly because of the inconsistency of voxel values due to the artefacts mentioned above [82].

Reliability of CBCT measurements is also a significant concern. As with conventional 2D cephalograms, point identification seems to be one of the largest sources of error. CBCT images, due to their 3D nature, present new challenges to the user, as multiple views of the dataset may be needed in order to identify a landmark, including 3D reconstructions and sections through the volume. Some points may even require new definitions; for example, the external auditory canal extends in depth and follows an oblique path, so Porion's traditional 2D definition needs updating [83]. Such difficulties reflect on repeatability; errors of measurement may exceed several degrees or mm, casting doubt on the capability of 3D measurements to reveal small treatment changes [84].

4.4.2 Soft Tissues

The geometry of the facial surface may be acquired from MRI or CT data if such data are available, but less invasive and costly methods that provide more accuracy and detail are recommended. Several techniques have been investigated, including laser scanning, structured lighting and photogrammetry [85, 86] (Fig. 4.8).

4.4.2.1 Laser Scanning

Laser scanning for 3D measurement and analysis of facial shape were introduced in orthodontics by the group of Moss in England [87–90]. Laser scanning of the head involves projecting a stripe of laser light and registering the shape of the stripe as it reflects from the three-dimensional surface. The stripe is usually projected as a vertical line and rotated around the face so that it scans the head from one side to the other. Scanning can be performed by movement of the laser and camera assembly

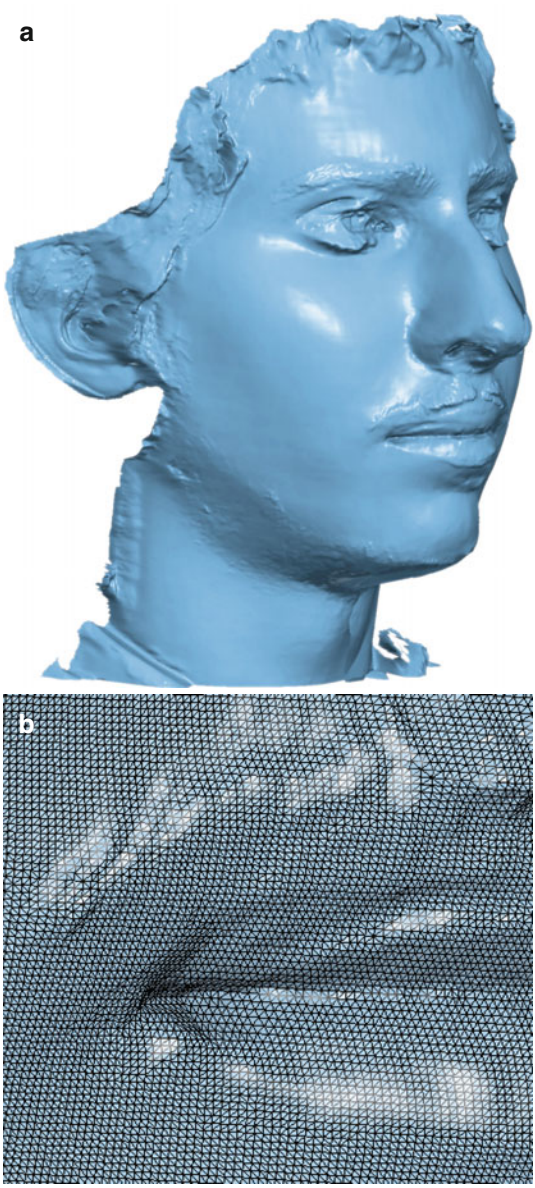

Fig. 4.8 (**a**) Facial surface as acquired by passive photogrammetry. (**b**) Detail of the corner of the mouth, showing size of triangular elements that constitute the surface

or by rotation of the patient seated on a motorised chair. Typical scans of the face may take 10–20 s. Other manufacturers use a horizontal laser stripe that scans the head vertically. This system is much faster than the rotational scan (less than 1 s) but requires multiple shots to acquire the whole face.

4.4.2.2 Structured Lighting

Structured lighting methods do not use a single laser stripe but project a complex light pattern over the whole object and acquire the 3D information from a single image. The main advantage of this method is the reduced exposure time, making it possible to register dynamic movements and facial expressions.

4.4.2.3 Photogrammetry

Photogrammetry uses two or more digital cameras to photograph the subject from different viewpoints. If the precise position of the cameras is known, then the location of each point of the subject's face in 3D space can be computed by simple triangulation, using data of the point's location on the images. The difficult part of this method is to identify corresponding points on the two images. Fortunately, skin has texture that allows matching between images, provided resolution and clarity are high enough. If texture is not sufficient, a random pattern can be projected on the face in order to facilitate correspondence search ('active' photogrammetry).

4.4.3 Dentition

Three-dimensional computer models of dental casts have many potential advantages. The reduced storage requirements may have been the first incentive to develop a 3D substitute of dental casts, but other benefits may prove more important. Models in electronic format can be retrieved faster than conventional ones and can be viewed on computer screens together with other electronic records. They allow transmission through the Internet for viewing at out-of-office locations and for sharing between doctors [91]. They enable virtual setups for treatment planning and can be used for fabrication of indirect bonding trays or other appliances and for guidance during bracket positioning [92, 93].

4.4.3.1 Hardware

Three-dimensional models can be created with a variety of methods, such as laser scanning, structured lighting, destructive scanning and CT scanning [94–96]. Differences between the methods relate to the accuracy and resolution, the time needed for a complete scan, the cost and simplicity of the procedure and the investment in equipment.

Laser scanning and structured lighting systems are relatively inexpensive and can be accomplished in a private office setting [96]. Both systems rely on projecting light (a laser beam or a pattern of dots or stripes) on the model and registering the reflected pattern by a single camera or two cameras. A major disadvantage is that multiple scans are usually required in order to acquire areas that are not visible to the projected light or the cameras from a single viewpoint. The individual scans then have to be "stitched" together by software in order to produce the final model, a process that may be time consuming. Another problem is that each model has to be processed individually and the method does not scale well to mass production. Intraoral scanning is an exciting possibility of this technology, as no impressions are

needed and view "stitching" is done automatically. The time factor is still an issue, as a complete scan may take several minutes.

Destructive scanning entails cutting thin slices of the models and scanning those. The 3D model is constructed by electronically stacking the individual slices. This method can give very detailed results and can be used for concurrent scanning of more than one model, but it is time consuming and the original model is destroyed in the process.

Use of CT scanning promises to cure most of the above shortcomings, but it is a process that requires expensive equipment. The level of detail may be lower than with some of the other methods, but progress in CT scanners may alleviate this problem. A major advantage is the simultaneous processing of many models and the possibility of scanning both plaster models and impressions.

4.4.3.2 Software

The final result of scanning is a computer file that contains the model of the dental casts as a collection of points in 3D space or as a triangular mesh surface. The utility of virtual dental casts depends heavily on the software for viewing and manipulating these surfaces. Current software enables viewing from any angle and at various zoom levels. Upper and lower dental casts can be viewed individually or in occlusion, and measurements of the teeth can be taken by marking points on the screen with the mouse. More sophisticated software allow isolation of individual teeth and their movement for the creation of virtual treatment setups (Fig. 4.9).

4.4.3.3 Clinical Use

A concern that has been raised in relation to the use of virtual models in place of the plaster ones is that it may be more difficult to perceive the anatomy from an image than from a true 3D object. Although software allows viewing from any angle and zooming to high detail, manipulation of the models is not as convenient as done by hand. Also, because haptic feedback is absent, it is not possible to assess the intercuspation between upper and lower teeth and get a feeling of occlusal contacts. Current computer interfaces do not seem to offer much hope for a satisfactory solution to this problem. Force-feedback devices are not sophisticated enough to simulate the complex contact between two plaster models, so the only present solution seems to be the adaptation of the orthodontist to the new medium. Currently available research indicates that treatment planning is not affected by the use of digital models [97].

Incentives to become accustomed to virtual models are the advantages that were mentioned above, including the creation of virtual diagnostic setups that are especially time consuming when performed on plaster casts. Virtual models are a practical necessity for construction of aligners for orthodontic treatment without brackets. They are also used for constructing transfer trays for indirect bonding, for automated wire bending and for feedback during direct bonding [93].

4.4.3.4 Accuracy

Accuracy of 3D digital models has been assessed by comparing measurements between plaster models and their digital counterparts. In general, digital models

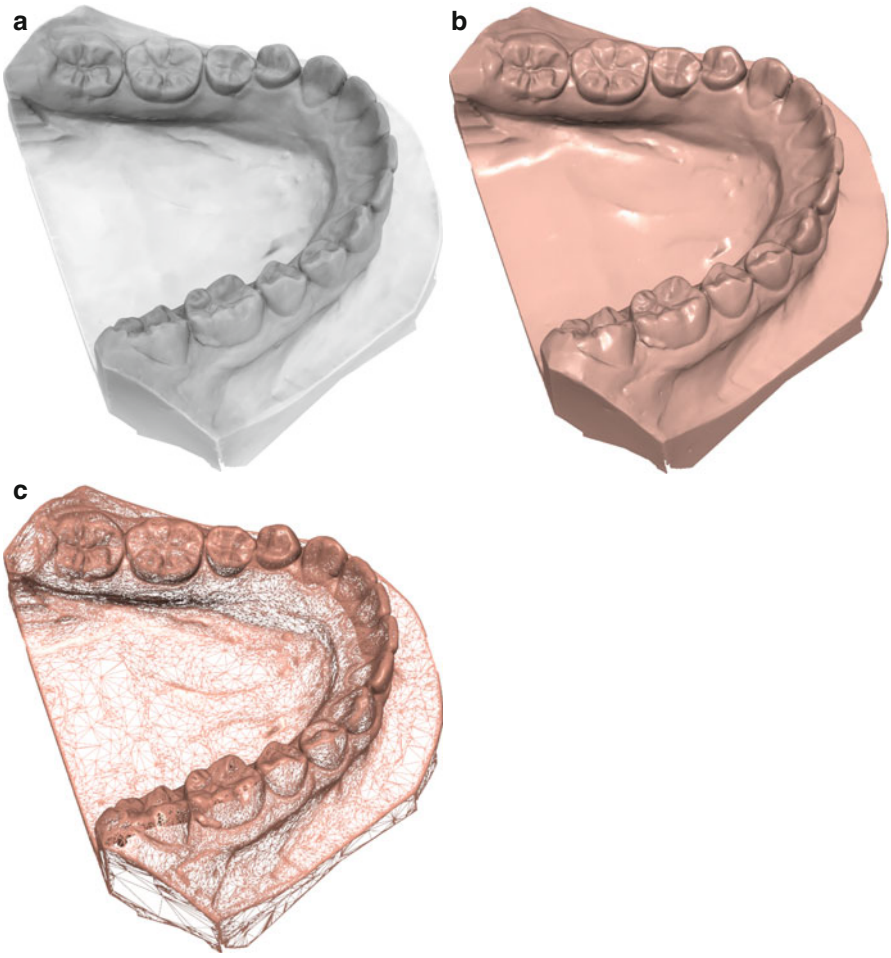

Fig. 4.9 Virtual models of dental casts rendered using different techniques. (**a**) Shading using ambient occlusion information, (**b**) shading using specular highlights to simulate glossy surface and (**c**) wireframe rendering to show level of detail

have been found to exhibit less accuracy and reproducibility [94, 98–100]. Some investigators reported systematic error, the digital models being smaller by about half a millimetre in all measurements [101], but this may have been because of alginate shrinkage during shipping or due to software problems [99]. Other systems have been found to be more accurate [94], but most investigators agree that any detected differences are not clinically significant for diagnosis and treatment planning [102]. In research settings, however, digital models need to be considered with caution, especially those produced by CT methods [98–100].

4.5 Simulation

Computer simulation is a rapidly expanding field in science. Simulation entails the construction of mathematical models that resemble their real counterparts, regarding their behaviour in specific circumstances. Simulation can be used for predicting the response of the real system, based on the calculations of a theoretical model that is known to apply, or for testing and refining theories, by comparing the behaviour of the model to the real data. In orthodontics, computer simulations can be used for research, education, treatment planning and patient information. Some of the current applications of computer simulation are discussed below.

4.5.1 Facial Soft Tissue Simulation

Facial simulation is a fast-moving research area, motivated partly by medical applications and partly by the film industry [103–108]. Various approaches are under development, and the details are mathematically and computationally rather involved and beyond the scope of this book. The basic principles are described in the following paragraphs.

Facial soft tissue simulation aims at constructing a computer model of the human face, including muscles and skin, so that simulation and prediction of orthodontic or surgical treatment is possible. This approach is different from the traditional predictions based on lateral cephalometric tracings in the following respects: (a) The computer model is three-dimensional, so it can be photorealistically rendered on the screen, with the skin having the texture and colour of the patient's face, and it can be rotated and viewed from whatever direction desired. (b) The response of the soft tissues to the surgical movement of the underlying hard tissues is not based on average ratios determined from previously studied patients. Instead, it is based on the physical properties of the soft tissues. (c) Muscles are also simulated, thus making it possible to view the face under varying expressions.

The model is composed of three parts, the skeletal unit, the muscles and the soft tissue covering. The skeletal unit is a model of the skeleton of the patient and is acquired from a CT scan. The skeletal unit is covered by a layer of simulated soft tissue, the outer surface of which is configured by data from a laser scan of the patient's face. Laser scanning equipment can digitise a large number of points on the skin surface in three dimensions and construct a representation of the face. The soft tissue layer is given the physical properties of actual soft tissues, so that it can respond to changes in the underlying skeletal unit or to pulling by simulated muscles embedded in it.

A simple model for simulating soft tissue is the mass-spring model. In this model, the soft tissue is represented as a collection of point masses connected by springs (Fig. 4.10). Some of the points are anchored on the skeletal unit, and they transfer any skeletal movements to the other points through the action of the springs. The outer points constitute the skin covering. Muscles are modelled as springs that connect skeletal units to soft tissue points or soft tissue points to soft tissue points and can contract and pull their endpoint towards each other.

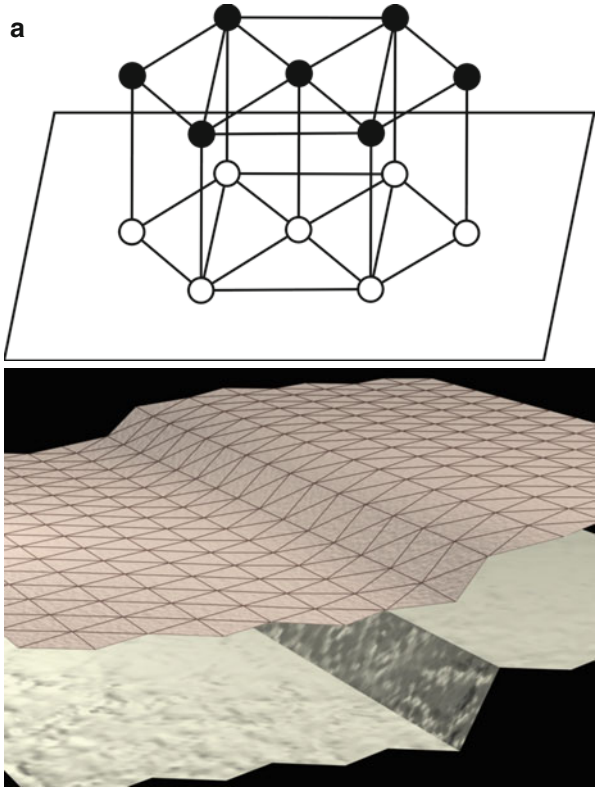

Fig. 4.10 Simulation model. (**a**) The spheres represent point masses that are connected by springs (only some are shown, as *straight lines*). *White spheres* are anchored to the osseous surface. *Black spheres* constitute the soft tissue surface. (b) Response of the model to simulated surgical movement of the skeletal surface. Even though the osseous surface has a sharp step, the overlying "skin" deforms smoothly, due to the elastic properties of the model. The grid on the "skin" shows the position of the individual triangular model elements, which extend down to the bone surface, but have been omitted for clarity

The main advantage of using such models of the soft tissues is that any changes in the underlying hard tissues should automatically result in accurate changes of the external facial shape. The model should be able to simulate changes due to functional mandibular movements (e.g. mouth opening and closing), orthodontic movements (e.g. incisor retraction) and surgical procedures. The 3D nature of the model makes it especially useful for predicting changes that cannot be modelled by the traditional 2D cephalometric methods, such as asymmetry cases and changes in the transverse dimension. Furthermore, because the model is physically based and simulates such behaviour of the soft tissues as elasticity and incompressibility, it should predict subtle effects such as soft tissue sagging and lip competence. The incorporation of muscle simulation opens the way for realistic prediction of facial dynamics [105, 109]. This should make it possible to predict the posttreatment aesthetics, not only in the neutral relaxed posture but during a smile or any other facial expression.

Facial simulation for surgical or orthodontic procedures is still in the experimental stages. Mainstream application in the orthodontic practice needs to overcome several obstacles. These include the added cost and radiation concerns of a CT scan for obtaining the underlying 3D skeletal geometry, the cost of obtaining a 3D laser scan of the facial surface and the development of easy to use software that is both

accurate enough for reliable predictions and fast enough for practical use. If these problems are overcome, then surgical planning should be able to provide significantly more help to the patient and doctor than current techniques.

4.5.2 Tooth – Alveolar – Periodontal Simulation

Simulation of teeth and periodontium is used for studying the response of these structures to loading, the pattern and magnitude of the generated stresses, the position of the centre of resistance and centre of rotation, the mechanical properties of the periodontal ligament and other variables. Most of the simulations use the technique of finite element (FE) analysis, where the simulated tooth and periodontium are subdivided into a large number of small units (elements). Each of these elements has simple mechanical properties requiring simple mathematical calculations, but taken together they can simulate complex geometric structures with nonlinear responses to applied forces. The literature contains several studies that have used this approach [110–116].

4.5.3 Wire Simulation: Biomechanics

Simulation of orthodontic wires is another field that has found application in orthodontic research and education. The behaviour of orthodontic loops under different conditions of activation is a subject of considerable interest. Laboratory testing is both time consuming and difficult [117], so testing on computer simulations provides valuable help. Computer simulations can be used for designing new loops, for investigating the force and moment properties of loops and for educational purposes.

Orthodontic wire simulation requires special considerations, because we are interested in large deformations. Therefore, equations from beam theory cannot be applied directly [118]. Finite element techniques, as used for the simulation of teeth and supporting structures, and other mathematical methods have been employed [119–122]. Surprisingly, although the theoretical considerations of orthodontic wire simulation are not especially challenging, very few software applications are currently available. Research into the biomechanical properties of loop designs and continuous archwires continues to be based on laboratory setups of force and moment sensors [123–128]. The most probable explanation is the lack of incentive from the clinical setting, due to the ever-increasing use of superelastic wires, and the related unpopularity of wire bending. This is unfortunate because reliable wire simulation methods could be coupled with periodontal simulation to construct a 3D “electronic typodont” that could be used both for research and educational purposes.

Figure 4.11 shows examples of activated loops and the resulting forces and moments, as predicted by a simulation program [120, 121]. The software allows the

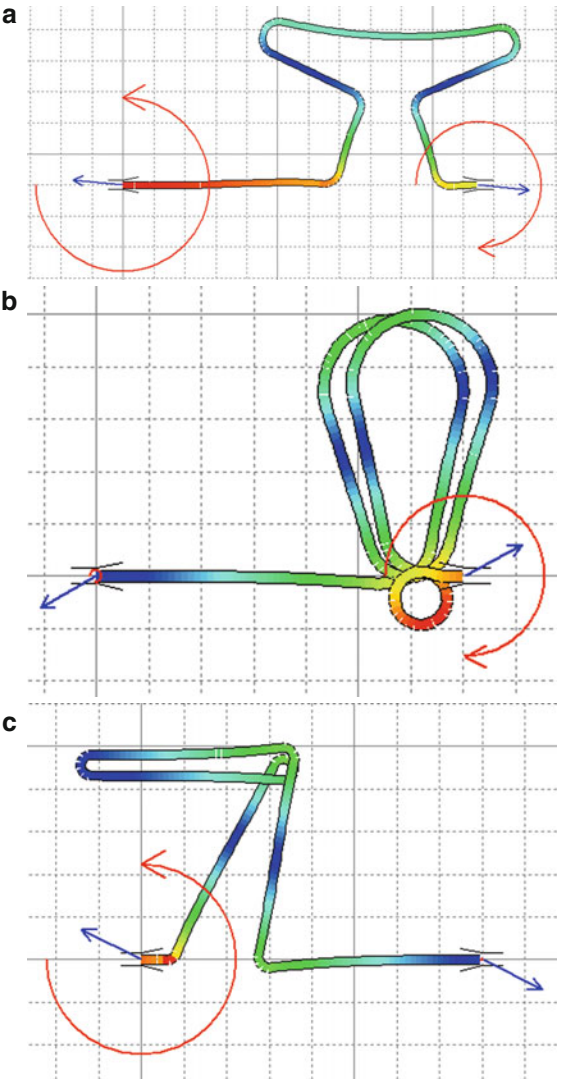

Fig. 4.11 Simulation of orthodontic loops. The loops are shown in the activation position, together with the forces and moments that are required for remaining at this configuration. Opposite forces and moments are applied by the loops on the two bracket positions. The loops are colour coded to show areas of low and high internal stress. The loops shown are (**a**) the T-loop, (**b**) the Gjessing loop [129] and (**c**) the Opus loop [127]

construction and evaluation of any loop design, but it is restricted to one plane of space, being a two-dimensional simulation. Therefore, the simulated loop is flat and cannot fully represent the designs that are used clinically. For example, in cases of canine retraction, the anti-rotation bends that are placed at the two ends of the loop cannot be simulated. Similarly, torquing moments resulting from twisting of the wire cannot be calculated. Otherwise, the software is easy to use and can be applied as a research and educational tool.

Conclusions

Computers have not only become ubiquitous but indispensable as well. Orthodontics, being a measurement-preoccupied specialty, is to benefit a lot from the application of computer-aided methods in clinical practice and research. For the time being, cephalometrics and imaging have been the most intense areas of development, but significant advances and explosive growth are shortly expected in 3D diagnostic systems and simulation. Knowledge in computer theory and practice is necessary for exploitation of the new methods. Postgraduate orthodontic programs will need to incorporate computer courses in their curriculum, in order to ensure that future researchers will be capable and proficient.

References

1. Battagel JM (1993) A comparative assessment of cephalometric errors. Eur J Orthod 15:305–314
2. Baumrind S, Frantz R (1971) The reliability of head film measurements: 1, landmark identification. Am J Orthod 60:111–127
3. Cohen AM (1984) Uncertainty in cephalometrics. Br J Orthod 11:44–48
4. Houston WJB (1983) The analysis of errors in orthodontic measurements. Am J Orthod 83:382–390
5. Houston WJB, Maher RE, McElroy D, Sherriff M (1986) Sources of error in measurements from cephalometric radiographs. Eur J Orthod 8:149–151
6. Sandler PJ (1988) Reproducibility of cephalometric measurements. Br J Orthod 15:105–110
7. Trpkova B, Major P, Prasad N, Nebbe B (1997) Cephalometric landmarks identification and reproducibility: a meta analysis. Am J Orthod Dentofacial Orthop 112:165–170
8. Damstra J, Huddleston Slater JJ, Fourie Z, Ren Y (2010) Reliability and the smallest detectable differences of lateral cephalometric measurements. Am J Orthod Dentofacial Orthop 138:546.e1–546.e8
9. Chan CK, Tng TH, Hagg U, Cooke MS (1994) Effects of cephalometric landmark validity on incisor angulation. Am J Orthod Dentofacial Orthop 106:487–495
10. Tng TT, Chan TC, Hagg U, Cooke MS (1994) Validity of cephalometric landmarks. An experimental study on human skulls. Eur J Orthod 16:110–120
11. Eriksen E, Solow B (1990) Linearity of cephalometric digitizers. Eur J Orthod 13:337–342
12. Tourne LPM (1996) Accuracy of a commercially available digitizer: a new method for assessment of errors in linearity. Angle Orthod 66:433–440
13. Gonzalez RC, Woods RE (2002) Digital image processing. Prentice Hall Inc., New Jersey
14. Halazonetis DJ (2004) What features should I look for in a scanner? Am J Orthod Dentofacial Orthop 125:117–118
15. Halazonetis DJ (2004) At what resolution should I scan cephalometric radiographs? Am J Orthod Dentofacial Orthop 125:118–119
16. Ongkosuwito EM, Katsaros C, van't Hof MA, Bodegom JC, Kuijpers-Jagtman AM (2002) The reproducibility of cephalometric measurements: a comparison of analogue and digital methods. Eur J Orthod 24:655–665
17. Held CL, Ferguson DJ, Gallo MW (2001) Cephalometric digitization: a determination of the minimum scanner settings necessary for precise landmark identification. Am J Orthod Dentofacial Orthop 119:472–481
18. Halazonetis DJ (2005) What do 8-bit and 12-bit grayscale mean and which should I use when scanning? Am J Orthod Dentofacial Orthop 127:387–388

19. Halazonetis DJ (2005) How can I eliminate noise in the dark areas when scanning radiographs or slides? Am J Orthod Dentofacial Orthop 127:83–84
20. Chadwick JW, Prentice RN, Major PW, Lam EW (2009) Image distortion and magnification of 3 digital CCD cephalometric systems. Oral Surg Oral Med Oral Pathol Oral Radiol Endod 107:105–112
21. Uysal T, Baysal A, Yagci A (2009) Evaluation of speed, repeatability, and reproducibility of digital radiography with manual versus computer-assisted cephalometric analyses. Eur J Orthod 31:523–528
22. Tsorovas G, Karsten AL (2010) A comparison of hand-tracing and cephalometric analysis computer programs with and without advanced features–accuracy and time demands. Eur J Orthod 32:721–728
23. Baumrind S, Miller DM (1980) Computer-aided head film analysis: the University of California San Francisco method. Am J Orthod 78:41–65
24. Macrì V, Wenzel A (1993) Reliability of landmark recording on film and digital lateral cephalograms. Eur J Orthod 15:137–148
25. Parker JR (1997) Algorithms for image processing and computer vision. Wiley, New York
26. Kazandjian S, Kiliaridis S, Mavropoulos A (2006) Validity and reliability of a new edge-based computerized method for identification of cephalometric landmarks. Angle Orthod 76:619–624
27. Dibbets JMH, Nolte K (2002) Effect of magnification on lateral cephalometric studies. Am J Orthod Dentofacial Orthop 122:196–201
28. Björk A, Skieller V (1983) Normal and abnormal growth of the mandible. A synthesis of longitudinal cephalometric implant studies over a period of 25 years. Eur J Orthod 5:1–46
29. Dryden IL, Mardia KV (1998) Statistical shape analysis. Wiley, Chichester
30. Lele S (1999) Invariance and morphometrics: a critical appraisal of statistical techniques for landmark data. In: Chaplain MAJ, Singh GD, McLachlan JC (eds) On growth and form. Spatio-temporal pattern formation in Biology. Wiley, New York
31. O'Higgins P (1999) Ontogeny and phylogeny: some morphometric approaches to skeletal growth and evolution. In: Chaplain MAJ, Singh GD, McLachlan JC (eds) On growth and form. Spatio-temporal pattern formation in Biology. Wiley, New York
32. Richtsmeier JT, Cheverud JM, Lele S (1992) Advances in anthropological morphometrics. Annu Rev Anthropol 21:283–305
33. Cakirer B, Dean D, Palomo JM, Hans MG (2002) Orthognathic surgery outcome analysis: 3-dimensional landmark geometric morphometrics. Int J Adult Orthodon Orthognath Surg 17:116–132
34. Singh GD, McNamara JA Jr, Lozanoff S (1998) Craniofacial heterogeneity of prepu-bertal Korean and European-American subjects with class III malocclusions: procrustes, EDMA, and cephalometric analyses. Int J Adult Orthodon Orthognath Surg 13:227–240
35. Singh GD, Clark WJ (2001) Localization of mandibular changes in patients with class II division 1 malocclusions treated with twin-block appliances: finite element scaling analysis. Am J Orthod Dentofacial Orthop 119:419–425
36. Halazonetis DJ (2004) Morphometrics for cephalometric diagnosis. Am J Orthod Dentofacial Orthop 125:571–581
37. Chatzigianni A, Halazonetis DJ (2009) Geometric morphometric evaluation of cervical vertebrae shape and its relationship to skeletal maturation. Am J Orthod Dentofacial Orthop 136:481.e1–481.e9
38. Bartzela T, Katsaros C, Rønning E, Rizell S, Semb G, Bronkhorst E, Halazonetis D, Kuijpers-Jagtman AM (2011) A longitudinal three-center study of craniofacial morphology at 6 and 12 years of age in patients with complete bilateral cleft lip and palate. Clin Oral Investig. doi:10.1007/s00784-011-0615-y
39. Moyers RE, Bookstein FL (1979) The inappropriateness of conventional cephalometrics. Am J Orthod 75:599–617
40. Halazonetis DJ (1999) Morphing and warping. Part I. Am J Orthod Dentofacial Orthop 115:466–470

41. Halazonetis DJ (1999) Morphing and warping. Part II. Am J Orthod Dentofacial Orthop 115:706–708
42. Gomes J, Darsa L, Costa B, Velho L (1999) Warping and morphing of graphical objects. Morgan Kaufmann Publishers Inc., San Francisco
43. Beier T, Neely S (1992) Feature-based image metamorphosis. ACM SIGGRAPH Comput Graph 26:35–42
44. Ackerman JL, Proffit WR (1995) Communication in orthodontic treatment planning: bioethical and informed consent issues. Angle Orthod 65:253–262
45. Fink B, Grammer K, Thornhill R (2001) Human (*Homo sapiens*) facial attractiveness in relation to skin texture and color. J Comp Psychol 115:92–99
46. Giddon DB, Sconzo R, Kinchen JA, Evans CA (1996) Quantitative comparison of computerized discrete and animated profile preferences. Angle Orthod 66:441–448
47. Halazonetis DJ (2002) Estimated natural head position and facial morphology. Am J Orthod Dentofacial Orthop 121:364–368
48. Lemley B (2000) Isn't she lovely? Discover 21:42–49
49. Perrett DI, Lee KJ, Penton-Voak I, Rowland D, Yoshikawa S, Burt DM, Henzi SP, Castles DL, Akamatsu S (1998) Effects of sexual dimorphism on facial attractiveness. Nature 394:884–887
50. Spyropoulos MN, Halazonetis DJ (2001) Significance of the soft-tissue profile on facial esthetics. Am J Orthod Dentofacial Orthop 119:464–471
51. Karavaka SM, Halazonetis DJ, Spyropoulos MN (2008) Configuration of facial features influences subjective evaluation of facial type. Am J Orthod Dentofacial Orthop 133:277–282
52. Ngan DC, Kharbanda OP, Geenty JP, Darendeliler MA (2003) Comparison of radiation levels from computed tomography and conventional dental radiographs. Aust Orthod J 19:67–75
53. Gijbels F, Sanderink G, Wyatt J, Van Dam J, Nowak B, Jacobs R (2003) Radiation doses of collimated vs non-collimated cephalometric exposures. Dentomaxillofac Radiol 32:128–133
54. Ludlow JB, Davies-Ludlow LE, Brooks SL (2003) Dosimetry of two extraoral direct digital imaging devices: NewTom cone beam CT and orthophos plus DS panoramic unit. Dentomaxillofac Radiol 32:229–234
55. Mah JK, Danforth RA, Bumann A, Hatcher D (2003) Radiation absorbed in maxillofacial imaging with a new dental computed tomography device. Oral Surg Oral Med Oral Pathol Oral Radiol Endod 96:508–513
56. European Commission (2004) Radiation protection 136. European guidelines on radiation protection in dental radiology. Luxembourg: Office for Official Publications of the European Communities. http://ec.europa.eu/energy/nuclear/radioprotection/publication/doc/136_en.pdf. Accessed 20 Jan 2012
57. Hujoel P, Hollender L, Bollen AM, Young JD, McGee M, Grosso A (2008) Head-and-neck organ doses from an episode of orthodontic care. Am J Orthod Dentofacial Orthop 133:210–217
58. Pauwels R, Beinsberger J, Collaert B, Theodorakou C, Rogers J, Walker A, Cockmartin L, Bosmans H, Jacobs R, Bogaerts R, Horner K, The SEDENTEXCT Project Consortium (2012) Effective dose range for dental cone beam computed tomography scanners. Eur J Radiol 81:267–271
59. Isaacson K, Thom A, Horner K, Whaites E (2008) Guidelines for the use of radiographs in clinical orthodontics. British Orthodontic Society, London
60. SEDENTEXCT (2011) Radiation protection: cone beam CT for dental and maxillofacial radiology. Evidence based guidelines 2011. http://www.sedentexct.eu/files/guidelines_final.pdf. Accessed 20 Jan 2012
61. Togashi K, Kitaura H, Yonetsu K, Yoshida N, Nakamura T (2002) Three-dimensional cephalometry using helical computer tomography: measurement error caused by head inclination. Angle Orthod 72:513–520
62. Williams FL, Richtsmeier JT (2003) Comparison of mandibular landmarks from computed tomography and 3D digitizer data. Clin Anat 16:494–500

63. Ludlow JB, Laster WS, See M, Bailey LJ, Hershey HG (2007) Accuracy of measurements of mandibular anatomy in cone beam computed tomography images. Oral Surg Oral Med Oral Pathol Oral Radiol Endod 103:534–542
64. Pinsky HM, Dyda S, Pinsky RW, Misch KA, Sarment DP (2006) Accuracy of three-dimensional measurements using cone-beam CT. Dentomaxillofac Radiol 35:410–416
65. Misch KA, Yi ES, Sarment DP (2006) Accuracy of cone beam computed tomography for periodontal defect measurements. J Periodontol 77:1261–1266
66. Marmulla R, Wortche R, Muhling J, Hassfeld S (2005) Geometric accuracy of the NewTom 9000 cone beam CT. Dentomaxillofac Radiol 34:28–31
67. Gribel BF, Gribel MN, Frazäo DC, McNamara JA Jr, Manzi FR (2011) Accuracy and reliability of craniometric measurements on lateral cephalometry and 3D measurements on CBCT scans. Angle Orthod 81:26–35
68. Berco M, Rigali PH Jr, Miner RM, DeLuca S, Anderson NK, Will LA (2009) Accuracy and reliability of linear cephalometric measurements from cone-beam computed tomography scans of a dry human skull. Am J Orthod Dentofacial Orthop 136:17.e1–17.e9
69. Lagravère MO, Carey J, Toogood RW, Major PW (2008) Three-dimensional accuracy of measurements made with software on cone-beam computed tomography images. Am J Orthod Dentofacial Orthop 134:112–116
70. Baumgaertel S, Palomo JM, Palomo L, Hans MG (2009) Reliability and accuracy of cone-beam computed tomography dental measurements. Am J Orthod Dentofacial Orthop 136:19–25
71. Barrett JF, Keat N (2004) Artifacts in CT: recognition and avoidance. Radiographics 24:1679–1691
72. Schulze R, Heil U, Gross D, Bruellmann DD, Dranischnikow E, Schwanecke U, Schoemer E (2011) Artefacts in CBCT: a review. Dentomaxillofac Radiol 40:265–273
73. Bryant JA, Drage NA, Richmond S (2008) Study of the scan uniformity from an i-CAT cone beam computed tomography dental imaging system. Dentomaxillofac Radiol 37:365–374
74. Katsumata A, Hirukawa A, Okumura S, Naitoh M, Fujishita M, Ariji E, Langlais RP (2007) Effects of image artifacts on gray-value density in limited-volume cone-beam computerized tomography. Oral Surg Oral Med Oral Pathol Oral Radiol Endod 104:829–836
75. Nackaerts O, Maes F, Yan H, Couto Souza P, Pauwels R, Jacobs R (2011) Analysis of intensity variability in multislice and cone beam computed tomography. Clin Oral Implants Res 22:873–879
76. Halazonetis DJ (2009) Commentary. Am J Orthod Dentofacial Orthop 136:25–28
77. Ballrick JW, Palomo JM, Ruch E, Amberman BD, Hans MG (2008) Image distortion and spatial resolution of a commercially available cone-beam computed tomography machine. Am J Orthod Dentofacial Orthop 134:573–582
78. Timock A, Cook V, McDonald T, Leo MC, Crowe J, Benninger B, Covell D (2011) Accuracy and reliability of buccal bone height and thickness measurements from cone-beam computed tomography imaging. Am J Orthod Dentofacial Orthop 140:734–744
79. Patcas R, Müller L, Ullrich L, Peltomäki T (2012) Cone-beam computed tomography and the anatomical reality of alveolar bone covering in the lower front. Am J Orthod Dentofacial Orthop 141:41–50
80. Leung CC, Palomo L, Griffith R, Hans MG (2010) Accuracy and reliability of cone-beam computed tomography for measuring alveolar bone height and detecting bony dehiscences and fenestrations. Am J Orthod Dentofacial Orthop 137(4 Suppl):S109–S119
81. Sun Z, Smith T, Kortam S, Kim DG, Tee BC, Fields H (2011) Effect of bone thickness on alveolar bone-height measurements from cone-beam computed tomography images. Am J Orthod Dentofacial Orthop 139:e117–e127
82. Nguyen E, Boychuk D, Orellana M (2011) Accuracy of cone-beam computed tomography in predicting the diameter of unerupted teeth. Am J Orthod Dentofacial Orthop 140:e59–e66
83. Ludlow JB, Gubler M, Cevidanes L, Mol A (2009) Precision of cephalometric landmark identification: cone-beam computed tomography vs conventional cephalometric views. Am J Orthod Dentofacial Orthop 136:312.e1–312.e10

84. Damstra J, Fourie Z, Huddleston Slater JJ, Ren Y (2011) Reliability and the smallest detectable difference of measurements on 3-dimensional cone-beam computed tomography images. Am J Orthod Dentofacial Orthop 140:e107–e114
85. Halazonetis DJ (2001) Acquisition of 3-dimensional shapes from images. Am J Orthod Dentofacial Orthop 119:556–560
86. Klette R, Schlüns K, Koschan A (1998) Computer vision. Three-dimensional data from images. Springer-Verlag Singapore Pte. Ltd., Singapore
87. Hennessy RJ, Moss JP (2001) Facial growth: separating shape from size. Eur J Orthod 23:275–285
88. Ismail SF, Moss JP, Hennessy R (2002) Three-dimensional assessment of the effects of extraction and nonextraction orthodontic treatment on the face. Am J Orthod Dentofacial Orthop 121:244–256
89. Moss JP, Linney AD, Grindrod SR, Arridge SR, Clifton JS (1987) Three-dimensional visualization of the face and skull using computerized tomography and laser scanning techniques. Eur J Orthod 9:247–253
90. Moss JP (2000) 2D or not 2D? That is the question. Am J Orthod Dentofacial Orthop 117:580–581
91. Marcel TJ (2001) Three-dimensional on-screen virtual models. Am J Orthod Dentofacial Orthop 119:666–668
92. Garino F, Garino B (2003) From digital casts to digital occlusal set-up: an enhanced diagnostic tool. World J Orthod 4:162–166
93. Redmond WJ, Redmond MJ, Redmond WR (2004) The OrthoCAD bracket placement solution. Am J Orthod Dentofacial Orthop 125:645–646
94. Bell A, Ayoub AF, Siebert P (2003) Assessment of the accuracy of a three-dimensional imaging system for archiving dental study models. J Orthod 30:219–223
95. Kuo E, Miller RJ (2003) Automated custom-manufacturing technology in orthodontics. Am J Orthod Dentofacial Orthop 123:578–581
96. Kusnoto B, Evans CA (2002) Reliability of a 3D surface laser scanner for orthodontic applications. Am J Orthod Dentofacial Orthop 122:342–348
97. Whetten JL, Williamson PC, Heo G, Varnhagen C, Major PW (2006) Variations in orthodontic treatment planning decisions of class II patients between virtual 3-dimensional models and traditional plaster study models. Am J Orthod Dentofacial Orthop 130:485–491
98. Tomassetti JJ, Taloumis LJ, Denny JM, Fischer JR Jr (2001) A comparison of 3 computerized Bolton tooth-size analyses with a commonly used method. Angle Orthod 71:351–357
99. Zilberman O, Huggare JAV, Parikakis KA (2003) Evaluation of the validity of tooth size and arch width measurements using conventional and three-dimensional virtual orthodontic models. Angle Orthod 73:301–306
100. Sjögren AP, Lindgren JE, Huggare JA (2010) Orthodontic study cast analysis–reproducibility of recordings and agreement between conventional and 3D virtual measurements. J Digit Imaging 23:482–492
101. Santoro M, Galkin S, Teredesai M, Nicolay OF, Cangialosi TJ (2003) Comparison of measurements made on digital and plaster models. Am J Orthod Dentofacial Orthop 124:101–105
102. Leifert MF, Leifert MM, Efstratiadis SS, Cangialosi TJ (2009) Comparison of space analysis evaluations with digital models and plaster dental casts. Am J Orthod Dentofacial Orthop 136:16.e1–16.e4
103. Koch RM, Gross MH, Carls FR, von Bueren DF, Fankhauser G, Parish YIH (1996) Simulating facial surgery using finite element models. In Computer Graphics Proceedings, Annual Conference Series, ACM SIGGRAPH, pp 421–428, doi: 10.1145/237170.237281
104. Koch RM, Roth SHM, Gross MH, Zimmermann AP, Sailer HF (2002) A framework for facial surgery simulation. Proceedings of ACM SCCG 2002, pp 33–42, doi: 10.1145/584458.584464
105. Lee Y, Terzopoulos D, Waters K (1995) Realistic facial modeling for animation. In: Computer graphics proceedings, annual conference series. ACM SIGGRAPH, Los Angeles, pp 55–62
106. Meehan M, Teschner M, Girod S (2003) Three-dimensional simulation and prediction of craniofacial surgery. Orthod Craniofac Res 6:102–107

107. Parke FI, Waters K (1996) Computer facial animation. A K Peters, Ltd., Wellesley
108. Teschner M, Girod S, Girod B (1999) Interactive osteotomy simulation and soft-tissue prediction. Proc Vision, Modeling, Visualization VMV'99, Erlangen, pp 405–412
109. Zhang Y, Prakash EC, Sung E (2002) Constructing a realistic face model of an individual for expression animation. Int J Inf Technol 8:10–25
110. Halazonetis DJ (1996) Computer experiments using a two-dimensional model of tooth support. Am J Orthod Dentofacial Orthop 109:598–606
111. Jeon PD, Turley PK, Ting K (2001) Three-dimensional finite element analysis of stress in the periodontal ligament of the maxillary first molar with simulated bone loss. Am J Orthod Dentofacial Orthop 119:498–504
112. Kawarizadeh A, Bourauel C, Jäger A (2003) Experimental and numerical determination of initial tooth mobility and material properties of the periodontal ligament in rat molar specimens. Eur J Orthod 25:569–578
113. Poppe M, Bourauel C, Jager A (2002) Determination of the elasticity parameters of the human periodontal ligament and the location of the center of resistance of single-rooted teeth a study of autopsy specimens and their conversion into finite element models. J Orofac Orthop 63:358–370
114. Rudolph DJ, Willes PMG, Sameshima GT (2001) A finite element model of apical force distribution from orthodontic tooth movement. Angle Orthod 71:127–131
115. Tanne K, Sakuda M, Burstone CJ (1987) Three-dimensional finite element analysis for stress in the periodontal tissue by orthodontic forces. Am J Orthod Dentofacial Orthop 92:499–505
116. Toms SR, Eberhardt AW (2003) A nonlinear finite element analysis of the periodontal ligament under orthodontic tooth loading. Am J Orthod Dentofacial Orthop 123:657–665
117. Vanderby R Jr, Burstone CJ, Solonche DJ, Ratches JA (1977) Experimentally determined force systems from vertically activated orthodontic loops. Angle Orthod 47:272–279
118. Beer FP, Johnston ER (1981) Mechanics of materials. McGraw-Hill, New York
119. DeFranco JC, Koenig HA, Burstone CJ (1976) Three-dimensional large displacement analysis of orthodontic appliances. J Biomech 9:793–801
120. Halazonetis DJ (1997) Design and test orthodontic loops using your computer. Am J Orthod Dentofacial Orthop 111:346–348
121. Halazonetis DJ (1998) Understanding orthodontic loop preactivation. Am J Orthod Dentofacial Orthop 113:237–241
122. Koenig HA, Burstone CJ (1974) Analysis of generalized curved beams for orthodontic applications. J Biomech 7:429–435
123. Bourauel C, Drescher D, Ebling J, Broome D, Kanarachos A (1997) Superelastic nickel titanium alloy retraction springs–an experimental investigation of force systems. Eur J Orthod 19:491–500
124. Chen J, Markham DL, Katona TR (2000) Effects of T-loop geometry on its forces and moments. Angle Orthod 70:48–51
125. Drescher D, Bourauel C, Thier M (1991) Application of the orthodontic measurement and simulation system (OMSS) in orthodontics. Eur J Orthod 13:169–178
126. Menghi C, Planert J, Melsen B (1999) 3-D experimental identification of force systems from orthodontic loops activated for first order corrections. Angle Orthod 69:49–57
127. Siatkowski RE (1997) Continuous arch wire closing loop design, optimization, and verification. Part I. Am J Orthod Dentofacial Orthop 112:393–402
128. Sifakakis I, Pandis N, Makou M, Eliades T, Bourauel C (2010) A comparative assessment of the forces and moments generated with various maxillary incisor intrusion biomechanics. Eur J Orthod 32:159–164
129. Gjessing P (1985) Biomechanical design and clinical evaluation of a new canine-retraction spring. Am J Orthod 87:353–362